This accepted article to IROS 2012 is made available by the authors in compliance with IEEE policy.
Please find the final, published version in IEEE Xplore, DOI: 10.1109/IROS.2012.6386150.

The X-Face: An Improved Planar Passive Mechanical Connector for Modular Self-Reconfigurable Robots

Nick Eckenstein and Mark Yim

***Abstract*— There is a need in the field of modular robotics for a low-profile docking face with a wide range of performance. Mechanical self-aligning geometry features for docking faces of modular reconfigurable robot systems can be varied to improve the reliability of connection systems. This paper presents a new two-layer mating face design for robots that are constrained to move in a plane. It has a provably larger area of acceptance than any to date. We present an analysis of both position and orientation misalignments with simulated results over a two parameter design space comparing this connector with two other best-in-class shapes. The results show an average acceptance area increase approximately 88% over gendered mating faces and approximately 138% over non-gendered mating faces.**

I. Introduction

Robots composed of multiple reconfigurable modular units are known as modular (and sometimes self-reconfigurable) robots. These robots are desirable for many reasons, including adaptability to new tasks, robustness through redundancy and self-repair. There has been a large amount of research in this area including dozens of hardware designs [1], [2]. These systems can be classified into three areas based on their reconfiguration style: *lattice* modules sit on a virtual fixed lattice and move and reconfigure from one lattice position to another; *chain* modules form chain and make and break loops to reconfigure; and *mobile* modules move on the environment and (un)dock with other modules or module clusters.

One of the defining elements of these systems is the connection system. The ability for modules to easily dock and undock with other modules is often the primary concern for modules in which reconfiguration is the primary function [3], [4]. For many chain style self-reconfiguring systems the docking process has been difficult to make consistent and reliable [5]–[8]. Primarily this occurs because of imprecision in the positioning and orientation of modules during the docking process.

Figure 1 shows the PolyBot G2 system which is a typical chain style self-reconfiguring system [9]. The module has a connection plate that is hermaphroditic, containing both 4 grooved pins, and 4 mating holes. Two connection plates mate by having the pins on one side dock with holes on the mating plate and vice versa. A shape memory alloy actuator grabs onto the grooves of the pins to latch the plates in place. Note that the ends of the pins are chamfered to accommodate small errors in positioning.

PolyBot G2 and G3 increases robustness in docking by providing extra sensing and control to help guide the docking process [5]. CONRO increases robustness by vibrating the connectors [7]. These techniques present a complexity and cost burden on computation and added sensing. A passive guiding mechanism is simpler and thus typically more robust and lower cost. For example, CKbot [10] and MTRAN-II [11] use magnetic connectors to aid positioning and orientation. Magnets tend to have a relatively short range of effect and are not as strong as physical connections (with comparable volume and mass).

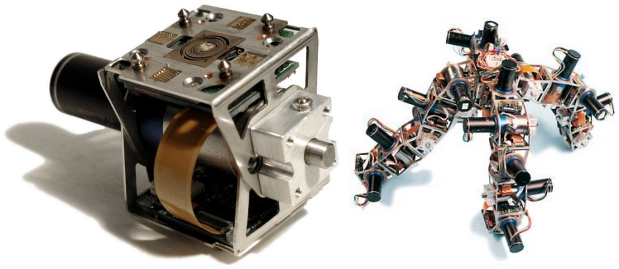

Fig. 1: PolyBot G2 module (left), 20 modules in a 4 legged spider configuration (right).

This paper introduces a new concept for self-aligning geometry called "X-Face". The current design applies to planar robots operating in SE(2) based on mechanical self-alignment. Examples of planar self-reconfigurable robots include [3], [12], [13]. This design promises a large **area of acceptance**. Area of acceptance is defined as the range of possible starting conditions for which mating will be successful. This area of acceptance is a geometric measure of the robustness of the docking process to errors in the relative position and orientation of two mating connectors.

A. Background

The alignment problem bears resemblances to a classic robotics problem: the peg-in-hole problem. The peg-in-hole problem requires precise alignment of two parts in position and orientation by a manipulator arm (represented by a number of pegs and holes, which are optionally chamfered).One solution is to use a Remote Center Compliance (RCC), first proposed by Nevins et al. [14].Whitney [15] applies an RCC device to the peg in hole problem and computes necessary equilibrium and RCC parameters for successful mating. Since then, RCC work has included different peg/hole shapes [16], sensing the hole using the arm [17], and six-DOF contact mechanics [18].

In the modular robotics community, there has been significant work on the docking mechanisms including sensor-based methods [5] and latching mechanisms [6]. Literature

Nick Eckenstein and Mark Yim, GRASP Lab and Department of Mechanical Engineering and Applied Mechanics, at University of Pennsylvania, email: neck @ seas.upenn.edu

on passive docking mechanisms, however is more sparse. Nilsson [19] defines a bound for 2D self-alignable offsets for position only, establishing bounds for both gendered and ungendered connectors. Modular robots, including Vasilescu and Rus et. al. [20], White and Lipson et. al. [21] sometimes make use of faces which have self-aligning features, but no comprehensive focus on these docking connectors has been done as yet. Furthermore, these robots often have a relatively small range of alignment in comparison to their size.

II. Setting Up the Problem

We assume that we have two modules that will mate together while being constrained to move on a plane. Since we focus primarily on the projected geometry of the module on the plane, we will refer to the modules as "faces." Furthermore, we assume one face (the moving face) is approaching a non-moving face (the base face). By changing frame of reference, we can make this equivalent to any general case of approaching faces. Problem specification includes face geometry, dynamic conditions (i.e. friction, damping, restitution coefficients), forcing condition, and degrees of freedom (DOF) of each face.

In general modular robots require some sort of mechanical latching in their interfaces to controllably hold or release. Since the faces occupy the same space once docked, these issues are the same regardless of face. We address just the docking leaving designing these latches to future work.

For our analysis we assume the robot arms hold both faces, and the arm holding the moving face moves in perfect position-controlled linear motion in the *forcing* direction (e.g. purely vertical) with the axis perpendicular to the direction of motion we call x and any initial offset position of one face from the mating face by x_0 (Fig. 3). Any initial offset in orientation from the mating angle we call θ_0. The arm holds each face at a fixed rotation point where the face is free to rotate. This is nearly equivalent to assuming the connector to be attached to an arbitrarily large robot by a pin joint. This is not unrealistic, as self-reconfiguration often occurs between large clusters of modules. We assume zero friction, zero coefficient of restitution and large enough damping so that inertial effects can be ignored. We also assume the forcing direction is such that the derivative of distance is negative, i.e. the faces must move towards each other to mate.

For the connectors in this paper, the design parameters we compare are the ratio $\frac{H}{D}$ (related to profile area HD), where D and H are the width and height of the face respectively, as seen in Fig. 2. The distance from the base of the connector profile to the rotation point (similar to the center of compliance), is r_p, a dimensionless number as a multiple of D. The design parameters scale with D, and we can objectively compare shapes regardless of size.

The problems under consideration in this paper are summarized in Table I.

Condition	State
Forcing:	$x = x_0$
Frictional:	Zero Friction
Damping:	Critically damped
Restitution:	Zero
Initial Offset Dimensions:	2 linear(x & y) and 1 angular (θ)
Free Dimensions:	1 angular ($theta$)
Base Face	Free in θ, Fixed in x & y

TABLE I: Mating condition summary

A. Face Types and Lateral Self-Alignment

In [19], Nilsson proves that for single-piece faces (faces which can be written as a function $y = f(x)$ in a plane, where y is the direction of motion to mate two matching faces), a face that gives the largest bi-directional offset correction possible for identical connectors is $D/3$ where $x(y_{max}) = D/3, x(y_{min}) = 2D/3$. He also proves that for gendered faces this relationship is $D/2$ where $x(y_{max})) = D/2$ for the male and correspondingly $x(y_{min}) = D/2$ for the female. We call these the S-Face and the V-Face respectively.

Figures 2 and 3 show the simplest example of the identical faces (S-Face), gendered faces (V-Face) and a newly proposed geometry (X-Face).

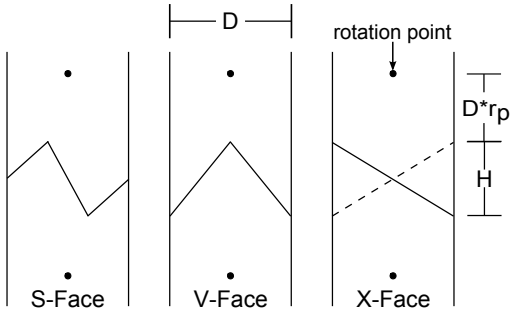

Fig. 2: Three face geometries with the same 'profile area'.

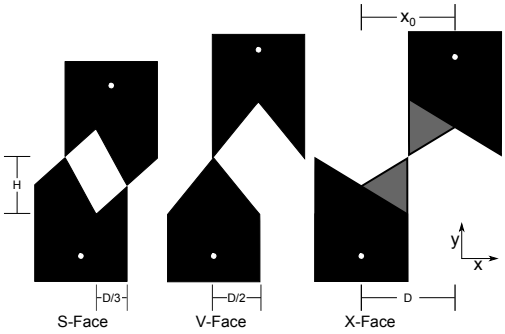

Fig. 3: A representation of the maximum lateral offset for successful self-alignment.

1) S-Face Geometry: The S-Face is the name we give to the identical face geometry analyzed by Nilsson. In this example we will use the simplest profile of the face (four vertices connected by straight line segments). Other geometries that have the same max and min conditions exist and similar analysis in this paper will apply without loss of generality. If the profile is viewed horizontally (as in Fig. 3) with horizontal width D, one vertex is at one-third of the way across the face, and the other is at two-thirds. The two

middle vertices are symmetrically offset from the vertical, one up and one down.

This shape gives the maximum lateral offset that still yields self-alignment for a 2D ungendered profile [19], an offset of $D/3$ in either direction.

2) V-Face Geometry: The V-face is the 2D equivalent of the cone and hole shape, a shape representing the maximal lateral offset for 2D profiles if we allow for the connectors to be gendered [19]. The male profile is essentially an isosceles triangle. The maximum lateral offset is $D/2$.

3) X-Face Geometry: The X-Face is a new face geometry designed to maximize acceptance range for real-world robots aligning in a SE(2) plane. It is composed of two layers, with the top a mirror image of the bottom, so it is no longer purely 2D, though the motions are still constrained to be planar. These faces will self-align in the lateral case as Nilsson examines it up to the full width D of the connector away, an improvement threefold over the S-face. Additionally, the X-Face does not suffer from the drawback of being gendered, meaning we do not have to check genders of faces before mating them. Since the self-alignment process is defined by contact of the two pieces, this is the theoretical maximum lateral offset for planar constrained motions of self-alignment.

B. Mating Problem Conditions

In the previous case we have assumed: planar constrained motion, the same size (D) for both connectors, no rotations when docking and the vertical axis as the docking direction.

III. Solving the Problem

A. X-Face

For the faces under consideration in this paper, the mating problem can be divided into three phases: the approach phase, the alignment phase, and the slide phase. During the approach phase, the parts approach along the direction of forcing until the first contact point is made. During the alignment phase, the parts rotate and slide relative to each other, maintaining contact until either the parts are either aligned with the same angle, or have misaligned beyond recovery. The final phase is the sliding phase, in which the parts that have the same rotational alignment slide into lateral agreement.

For the following analysis, we exclude cases where two approaching faces will not contact. When the forcing direction is along the $y - axis$, this is equivalent to $x_0 > 2D * r_p + H$. We call this the "distance condition", and it applies to all connectors.

1) Approach Phase: The approach phase ends when contact occurs, which can be handled by applying collision detection. This gives us the point of first contact.

2) Alignment Phase: When the first point contact is made, generically we will assume a vertex on one side contacts a line segment on the other side. The next step is to determine how the parts will rotate; towards alignment or away from alignment.

The direction of relative rotation can be determined by the geometry; the location of each rotation point (where the robot arm is applying translational forces but no torques) call them P_M and P_B, the location of the point of contact P_C and the normal to the line segment at the point of contact.

We assume a system without friction, so the only forces on both bodies at P_C must be in the direction normal to the line at P_C and in equal and opposite directions.Since the moving face must rotate about P_M the force at P_C will cause a torque about P_M which will indicate its rotation direction. Similar analysis can be used for the base face. In addition to this torque, a slip occurs at P_C. The complication comes from the fact that both the contact slope and the location of P_C changes as motion occurs and in some cases the motion can reverse.

We model this by building a simplified dynamic system (with moment of inertia $I_1 = I_2$ arbitrarily small, but nonzero) seen in Fig. 4. We numerically integrate this system to simulate the alignment phase. We only care about the path and not the rate, so the actual magnitudes of I and F do not matter, and are excluded by setting them to 1:

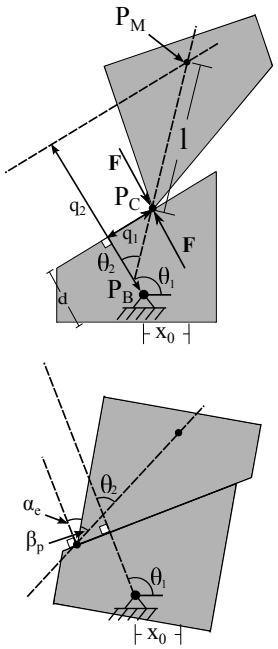

Fig. 4: Alignment path

$$\begin{aligned} q_2 &= d + l\cos(\theta_2) \\ \ddot{\theta_1} &= -q_1 \\ (\ddot{\theta_1} - \ddot{\theta_2}) &= -\sin(\theta_2)l \end{aligned} \tag{1}$$

Together with the forcing condition $x = x_0$, this defines a one-DOF system.

The alignment condition is:

$$\theta_2 = \beta_p + \alpha_e \tag{2}$$

where β_p and α_e are constant angles determined by the face geometry as shown in Fig. 4. β_p is the angle between the point face lever arm and its vertical. α_e is the angle between

the edge normal and the edge face vertical. Misalignment conditions occur if $\theta_2 < 0$. This represents a *bad mate*, which we will talk more about shortly.

3) Sliding Phase: Once the faces are aligned, we move into the sliding phase. During the sliding phase, the two pieces are aligned (that is, $\theta_{moving} = \theta_{fixed}$), but there remains some (x,y) offset. Since we have excluded those situations which do not meet the "distance condition", we know that these two faces will at some point be close enough to dock. We also know that the derivative of the distance is negative, so the faces can only get closer. Aligned faces represent a stable equilibrium, so the only way for them to get closer is by sliding into the mating position. Thus, if we satisfy the alignment condition and the distance condition, we have a successful mate.

Likewise, a pair of faces which has failed to meet the alignment condition must necessarily be a failure. Even if it gets close enough, we will only get a "bad mate", which the system will not be able to recover from if the forcing condition is a constant.

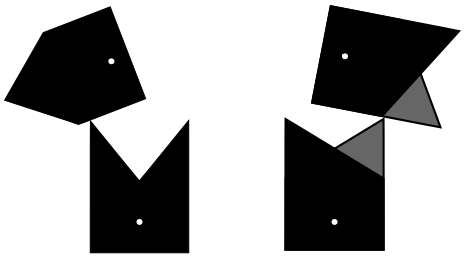

Fig. 5: Examples of bad mates. Bad mates are unrecoverable for constant forcing conditions.

B. V-Face and S-Face

The earlier collision model is fine when only one-point and sliding contact cases are possible, as in the case of the X-Face. The S-face and V-face are slightly more complicated; there exists for these models a two-point contact case, as seen in Fig. 6. Rather than attempt to solve these cases, we establish bounds for these faces beyond which they will certainly fail. These characteristics give us an outer bound or "best case" on area of acceptance to compare to the X-Face simulation.

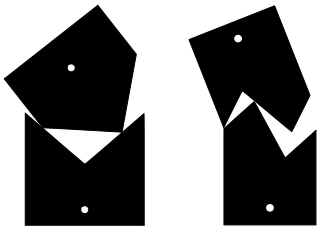

Fig. 6: Example of two-point contact case.

The "best case" bounds for these faces are defined as follows. The path of the maximal point (e.g. the tip) of the moving face must contact one of the faces on the mating shape which would be adjacent to it in the mating minimal point. For the V-Face, this is mathematically equivalent to:$|x_{tip}| < D/2$. The other condition is that the initial angular offset does not already break the misalignment condition; meaning $|\theta_0| < \frac{pi}{2} - |\alpha_e|$.

IV. Results

We ran the numerical simulator on the X-, S-, and V-Faces over a range of parameters. The relevant parameters here, as mentioned in Section II-B, are $\frac{H}{D}$ and r_p. We tested each face over the same subset of the feasible set of initial states $\{-D < x_0 < D, -\frac{pi}{2} < \theta_0 < \frac{pi}{2}\}$. The subset of initial conditions is a combination of 41 x_0 values and 41 θ_0 values, giving us 1681 discrete points evenly spaced over both dimensions of the feasible area. Running the simulation on each of these points gives us a set of initial conditions paired with their successful/failed state. We use the number of successful conditions as a metric M for that particular connector.

These metrics were generated for several values of the design parameters $\frac{H}{D}$ and r_p. M serves as a scalar discretized approximation of the area of acceptance we can use for comparison. We present the these metrics and their ratios in the Tables II-IV.

For the X-Face, the simulator was run once for each layer, comparing distances to see which layer collides first.

We can see that the X-Face generates a larger area of acceptance for most values in the design space. Some parameter values give better results with the "best case" of V or S-Face, but only in a specific narrow range. If we take the mean across the design space, we find that the mean X-Face/V-Face ratio is 1.8838, and the mean X-Face/S-Face ratio is 2.3846. In almost every case of H/D and r_p the X-Face has significant improvement over both S-Face and V-Face area of acceptance. The few exceptions are near $r_p = 0$ and $H/D = 1$.

A. Discussion

Looking at the data, we see some unintuitive results. As the rotation point comes closer to the face, the area of acceptance increases as we expect, however it drops off for $r_p = 0$. This is because of the distance condition; Once the rotation point is that close, significant offsets will result in failed mates simply because the faces do not come close enough together. As the $\frac{H}{D}$ ratio increases, the area of acceptance across all faces decreases. As mentioned for the "best case", there is some angular offset limit beyond which docking cannot succeed. Increasing the slope $\frac{H}{D}$, reduces this limit, naturally depressing the area of acceptance. More extreme values of $\frac{H}{D}$ and r_p were examined, but the area of acceptance "plateaus" and ceases to be interesting.

The authors recognize that the metric used in this paper is not necessarily ideal; correcting for errors in position and orientation is done over a range. We desire some metric that gives a range of $\{x_0, \theta_0\}$ offsets that will always succeed rather than a total count of all places where this is possible.

	r_p values										
H/D	0	1	2	3	4	5	6	7	8	9	10
0.0625	659	820	687	511	403	327	283	248	223	204	186
0.10882	623	802	667	501	395	322	281	246	222	200	186
0.18946	545	763	649	480	387	319	276	243	219	199	179
0.32988	397	696	618	440	371	307	269	239	216	195	176
0.57435	206	545	587	385	344	292	256	232	208	189	173
1	67	318	459	305	303	262	234	210	192	173	157
1.7411	41	120	254	274	214	206	187	165	146	126	108
3.0314	80	119	163	229	173	138	135	131	123	112	102
5.278	89	107	124	142	131	115	105	91	89	88	84
9.1896	74	75	89	92	89	87	82	79	76	72	69
16	55	57	62	63	64	63	68	61	59	60	57

TABLE II: M(X-Face)

	r_p values										
H/D	0	1	2	3	4	5	6	7	8	9	10
0.0625	37	739	598	403	282	224	186	159	142	125	114
0.10882	105	699	570	392	278	222	185	159	139	125	114
0.18946	93	619	519	379	273	217	181	156	138	125	114
0.32988	182	518	452	354	263	211	178	153	136	123	109
0.57435	209	379	353	303	249	200	172	150	132	120	109
1	208	239	236	223	204	183	161	142	126	114	105
1.7411	159	159	159	156	150	143	133	126	116	107	99
3.0314	99	99	99	99	99	97	95	93	90	87	84
5.278	59	59	59	59	59	59	59	59	59	58	58
9.1896	39	39	39	39	39	39	39	39	39	39	39
16	19	19	19	19	19	19	19	19	19	19	19

TABLE III: M(V-Face)

	r_p values										
H/D	0	1	2	3	4	5	6	7	8	9	10
0.0625	38	508	448	256	178	143	116	100	87	76	73
0.10882	108	480	425	251	176	141	115	98	87	77	73
0.18946	99	444	389	245	170	135	113	98	85	77	73
0.32988	203	387	341	227	165	129	112	96	84	75	68
0.57435	193	292	272	207	155	128	106	95	82	74	67
1	179	200	193	172	143	116	101	87	77	73	64
1.7411	133	130	133	127	116	102	90	81	73	67	61
3.0314	80	80	83	80	79	75	71	71	64	60	54
5.278	52	53	54	53	53	52	52	51	49	48	49
9.1896	26	27	26	27	26	26	27	26	27	26	26
16	26	27	26	26	27	26	26	26	26	27	26

TABLE IV: M(S-Face)

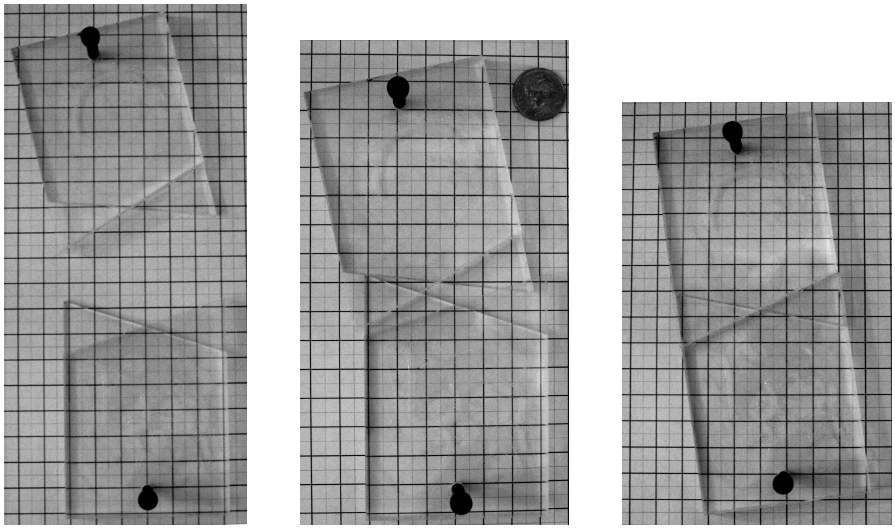

(a) Before alignment (b) During alignment (c) After alignment

Fig. 7: Example of experimental validation procedure for X-Face with x_0=2cm, $\theta_0 = arctan(\frac{1}{3}) \simeq 0.32$. The grid pattern behind the transparent pieces has a 0.5cm spacing.

B. Experimental Validation

Ideally, we would fully validate the results experimentally; however given the scale involved in calculating the area of acceptance for these connectors, it is difficult to address this over the full range examined in the tables. Each design has 1681 initial conditions that are checked for acceptance, for 100 different combinations of design parameters for each face type. Additionally, some conditions (no friction, coef. of restitution) are impractical to replicate in the lab.

Simple experimental validation was performed by constructing small models of the faces and manually driving them together. Offsets (translational, and angular measured by tangent) are measured by use of grid paper beneath the models. Fig. 7 shows a typical run. The validation generally agreed with the model, except in cases where static friction became significant. In these cases the models were observed to "stick" and not move along the prescribed path. To find M for the equivalent real-world case models, we would need to add friction to our model.

C. Limitations and Issues

The possibility exists in the real world case for some misalignment in the out-of-plane direction. A small design change can fix this misalignment. Taller layers and a gap between layers adds some tolerance to out-of-plane misalignment by keeping the appropriate layers in contact. This prevents small misalignments from causing complete failure to engage the connectors correctly. Future work includes applying the X-face concept to improving the acceptance range of three-dimensional connectors.

The lack of friction in the analysis is problematic. In particular, stiction often leads to jamming failure. Friction may have significant implications; steeper connectors may have wider area of acceptance in high-friction cases. Dynamic friction is also capable of exerting an influence in terms of relative alignment speed of the two faces. A more general simulator which can account for cases with more than one contact point and/or friction could be helpful in fully determining the viability of different connector shapes and is left to future work.

V. Conclusion

This paper presents a new face shape, the X-Face that has triple the previously largest acceptance distance for planar genderless connectors. *Acceptance area* is explored which includes angle as well as position misalignments. A simulator is used to find an area of acceptance over a two design parameter set of values for the new face. Over a representative set of the relevant design parameters (profile size, remoteness of center of rotation), with a few exceptions, the X-Face was found to have a significantly greater area of acceptance. The mean across all the cases examined is found to be $\sim$88% greater for the X-Face compared to the V-Face, and $\sim$138% greater for the X-Face compared to the S-Face. The S-Face and X-Face are the ungendered faces, so for cases where we require genderless docking such as modular self-reconfigurable robotics, we believe this represents a significant improvement in capture capability for low-profile docking faces.

References

[1] M. Yim, W. Shen, B. Salemi, D. Rus, M. Moll, H. Lipson, E. Klavins, and G. Chirikjian, "Self-Reconfigurable Robot Systems," *IEEE Robotics & Automation Magazine*, p. 44, 2007.

[2] K. Støy, *An Introduction to Self-Recongurable Robots*. Boston, MA: MIT Press, 2009, to appear.

[3] D. Rus and M. Vona, "Self-reconfiguration planning with compressible unit modules," in *Proc. of the IEEE Intl. Conf. on Robotics and Automation*, Detroit, 1999.

[4] S. Murata, H. Kurokawa, and S. Kokaji, "Self-assembling machine," in *Proc. IEEE Int. Conf. on Robotics and Automation*, San Diego, California, May 1994.

[5] K. Roufas, Y. Zhang, D. Duff, and M. Yim, "Six degree of freedom sensing for docking using ir led emitters and receivers," *Experimental Robotics VII*, pp. 91–100, 2001.

[6] W. Shen, R. Kovac, and M. Rubenstein, "Singo: a single-end-operative and genderless connector for self-reconfiguration, self-assembly and self-healing," in *Robotics and Automation, 2009. ICRA'09. IEEE International Conference on*. IEEE, 2009, pp. 4253–4258.

[7] W. Shen and P. Will, "Docking in self-reconfigurable robots," in *Intelligent Robots and Systems, 2001. Proceedings. 2001 IEEE/RSJ International Conference on*, vol. 2. IEEE, 2001, pp. 1049–1054.

[8] M. Nilsson, "Connectors for self-reconfiguring robots," *Mechatronics, IEEE/ASME Transactions on*, vol. 7, no. 4, pp. 473–474, 2002.

[9] M. Yim, D. Duff, and K. Roufas, "Polybot: a modular reconfigurable robot," in *Proc. of the IEEE Intl. Conf. on Robotics and Automation*, San Francisco, April 2000.

[10] M. Yim, B. Shirmohammadi, J. Sastra, M. Park, M. Dugan, and C. Taylor, "Towards robotic self-reassembly after explosion," in *Intelligent Robots and Systems, 2007. IROS 2007. IEEE/RSJ International Conference on*, 2007, pp. 2767–2772.

[11] S. Murata, E. Yoshida, K. Tomita, H. Kurokawa, A. Kamimura, and S. Kokaji, "Hardware design of modular robotic system," in *Proc. IEEE/RSJ Int. Conf. on Intelligent Robots and Systems*, Takamatsu, Japan, October 2000.

[12] J. Bishop, S. Burden, E. Klavins, R. Kreisberg, W. Malone, N. Napp, and T. Nguyen, "Programmable parts: A demonstration of the grammatical approach to self-organization," in *Intelligent Robots and Systems, 2005.(IROS 2005). 2005 IEEE/RSJ International Conference on*. IEEE, 2005, pp. 3684–3691.

[13] M. Tolley, V. Zykov, H. Lipson, and D. Erickson, "Directed fluidic self-assembly of microscale tiles," *Micro-Total Analysis Systems (uTAS)*, pp. 1552–1554, 2006.

[14] J. Nevins, "Exploratory research in industrial modular assembly," C.S. Draper Laboratory, MA, Tech. Rep. R-800, Mar 1974.

[15] D. E. Whitney, "Quasi-static assembly of compliantly supported rigid parts," *Journal of Dynamic Systems, Measurement, and Control*, vol. 104, no. 1, pp. 65–77, 1982. [Online]. Available: http://link.aip.org/link/?JDS/104/65/1

[16] F. Dietrich, D. Buchholz, F. Wobbe, F. Sowinski, A. Raatz, W. Schumacher, and F. Wahl, "On contact models for assembly tasks: Experimental investigation beyond the peg-in-hole problem on the example of force-torque maps," in *Intelligent Robots and Systems (IROS), 2010 IEEE/RSJ International Conference on*, oct. 2010, pp. 2313 –2318.

[17] H. Bruyninckx, S. Dutre, and J. De Schutter, "Peg-on-hole: a model based solution to peg and hole alignment," in *Robotics and Automation, 1995. Proceedings., 1995 IEEE International Conference on*, vol. 2, may 1995, pp. 1919 –1924 vol.2.

[18] T. Meitinger and F. Pfeiffer, "The spatial peg–in–hole problem," *IEEE/RSJ Cong. on Intelligent Robots & Systems, VolIII*, 2007. [Online]. Available: http://citeseerx.ist.psu.edu/viewdoc/summary?doi=?doi=10.1.1.18.8685

[19] M. Nilsson, "Symmetric docking in 2d: A bound on self-alignable offsets," in *IASTED '99: Robotics and Automation*, Oct. 1999.

[20] I. Vasilescu, P. Varshavskaya, K. Kotay, and D. Rus, "Autonomous modular optical underwater robot (amour) design, prototype and feasibility study," in *Robotics and Automation, 2005. ICRA 2005. Proceedings of the 2005 IEEE International Conference on*, april 2005, pp. 1603 – 1609.

[21] P. White, V. Zykov, J. Bongard, and H. Lipson, "Three dimensional stochastic reconfiguration of modular robots," in *Robotics: Science and Systems*, Cambridge, 2005, pp. 161–168.